Local SAR Calibration and Prediction Model in Parallel Transmit MRI

L. Alon[1], C. M. Deniz[1], R. Lattanzi[1], G. Wiggins[1], R. Brown[1], D. K. Sodickson[1,2], and Y. Zhu[1]

[1]Center for Biomedical Imaging, Department of Radiology, NYU School of Medicine, NYU School of Medicine, New York, NY, United States, [2]Sackler Institute of Graduate Biomedical Sciences, NYU School of Medicine, New York, NY

Introduction: It was shown by Zhu (1) that the local RF power deposition following a parallel excitation with multiple coils can be calculated once the local electric field covariance matrix Λ_r is known. Local SAR at the *r*-th position is given by (1):

$$\text{Local SAR}(r) = [w_1 \ldots w_m]^H \left(\left(\frac{\sigma(r)}{2\rho(r)} \right) \begin{bmatrix} \varepsilon_1(r) \\ \vdots \\ \varepsilon_m(r) \end{bmatrix}^* [\varepsilon_1(r) \ldots \varepsilon_m(r)] \right) \begin{bmatrix} w_1 \\ \vdots \\ w_m \end{bmatrix} = \omega^H A_r \omega$$

Where σ is the conductivity of the sample, ρ is the proton density of the sample, ε_i is the electric field generated by *i*-th coil at position *r*, w_i is the complex valued prescribed pulse in *i*-th coil where ^{H} represents the complex-conjugate transpose. In this study, we employ the equation above for the calibration and prediction of local SAR, both in simulation and in a phantom. Based on eq(1), once Λ_r is calibrated, we have the capacity to predict the local SAR for any RF pulses played out on the parallel transmit setup. The calibration process is described in this abstract, as well as the prediction of temperature change resulting from the local SAR prediction model. This local SAR prediction approach extends previous work on in vivo global SAR calibration and prediction [1,3].

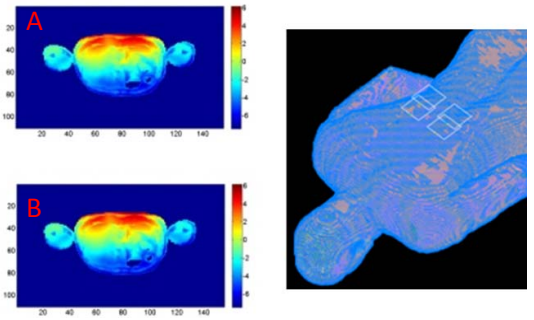

Figure 1. A. Log of SAR simulated using FDTD. B. Log of Predicted SAR. C. Human mesh and coil setup used for simulation

Theory and Methods: The heat equation for a non-perfused material with a heat source is[3]. (2): $\rho \cdot c \frac{\partial T}{\partial t} = \nabla \cdot (k \nabla T) + SAR\rho$. Where ρ is the material density *c* is the heat capacity, *T* is the temperature, *k* is the thermal conductivity and *t* is the time. Since thermal conduction requires time and a temperature gradient to affect the temperature distribution, thermal conduction can be neglected for a short period after initiation of heating [3], yielding (3): $\Delta T(r) \propto SAR(r)$. Assuming temperature change is in the linear regime, Eq. (3) allows the local SAR prediction model to be calibrated using the temperature difference maps acquired via the MR thermometry proton resonance frequency shift (PRF) method. Temperature maps are calculated from phase-difference maps calculated using the following equation [3] (4): $\Delta T = \frac{\Delta\phi}{\alpha \cdot TE \cdot \omega}$. Where α=0.01ppm/°C is the PRF change coefficient, ϕ is the phase difference, ω is the Larmor frequency at 7T. Simulation: A four surface coil parallel transmit setup was modeled on a human body mesh (Figure 1) using commercially available FDTD software (xFDTD, Remcom, PA, USA). Since Λ_r is a complex-Hermitian matrix, m^2 unknown variables (where *m* is the number of transmit coils) must be solved to determine the Λ_r matrix entries. Correspondingly, 16 FDTD simulations were conducted with different prescribed coil drive current amplitudes and phases. SAR maps generated by xFDTD were then used to obtain the entries of Λ_r on a voxel-by-voxel basis using a linear least squares fit. SAR distribution was then predicted using Equation (1) and random set of coil currents. Identical weights were then used to run an additional simulation and the resulting SAR map was compared with the predicted one (Figure 1). Phantom Study: To assess the model in a practical MR environment, experiments were performed on a 7T Siemens scanner (Siemens Medical Solutions, Erlangen, Germany) equipped with an 8-channel parallel transmit system. An 2.5Liter agar gel phantom was created using 18grams/L agar and 9grams/L NaCl to increase conductivity and facilitate RF induced heating. The T_2^* value of the phantom was ~23.1ms. Compartmental tubes allowed temperature probes to make direct contact with the gel in at various locations within the phantom. Three insulated surface coils were placed around the phantom to generate RF heating. As an experimental control three oil phantoms with zero conductivity, and hence immune to RF heating, were introduced to measure phase drift of the MR system (figure 2-B). In this three coil experiment, 9 heating experiments were conducted to estimate the entries of the Λ_r matrix. Phase images were acquired prior and subsequent to a heating sequence (Figure 2A). The phase images were then subtracted and unwrapped to produce temperature change map using equation (4). (Figure 3 shows the heating weightings). A 2D spoiled GRE sequence with the following parameters was used for phase map acquisition: TE=15ms, TR=50ms, number of signal averages=4, Flip angle=30 degrees, slice thickness=5mm, matrix size= 128x128. The acquisition total time was 27 seconds. For the heating sequence, a GRE sequence with a TR=4.1, flip angle=60 degrees and total acquisition time=303 seconds. Before conducting our local SAR calibration experiment we confirmed that heating due to the heating sequence is conducted within the linear range of temperature change using Luxtron fluoroscopic MR-compatible optical temperature probes. We also confirmed that the MR thermometry temperature maps agreed with the temperature measure with the probes. The calculated temperature maps were then used to fit our linear model such that the coefficients of Λ_r were determined. We then applied a set of random currents for each of the coils and ran the heating sequence. Once more, we acquired phase maps before and after the heating to generated a temperature-difference map. We then compared our measured temperature-change using the PRF method with the predicted temperature-change calculated using equation (1) and the set of random currents (figure 4).

Exp	Coil 1 Mag	Coil 1 Phase (deg)	Coil2 Mag	Coil2 Phase (deg)	Coil3 Mag	Coil3 Phase (deg)
1	1	0	0	0	0	0
2	0	0	1	0	0	0
3	0	0	0	0	1	0
4	1	0	1	0	0	0
5	1	0	1	90	0	0
6	0	0	1	0	1	0
7	0	0	1	0	1	90
8	1	0	0	0	1	0
9	1	0	0	0	1	90
10	1	59.248	0.3	157.98	0.6	100.32

Figure 3. Amplitude phase weights applied to each of the coils during 9 experiments for the calibration of Λ_r and 1 experiment for testing the prediction of the local SAR while applying random weights.

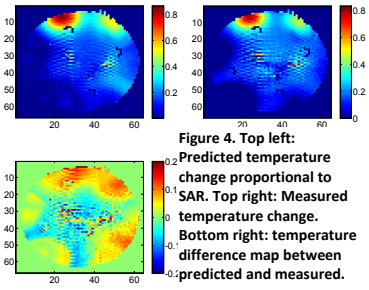

Figure 4. Top left: Predicted temperature change proportional to SAR. Top right: Measured temperature change. Bottom right: temperature difference map between predicted and measured.

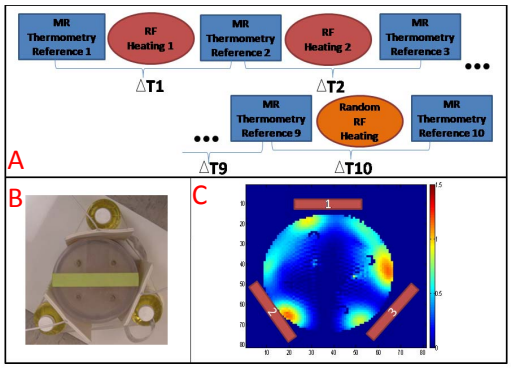

Figure 2. A. Diagram of temperature acquisition scheme using MR thermometry -PRF method. Before and after each heating sequence, phase reference images are taken and temperature maps are created. B. Image of the phantom used with the coils around it and 3 oil bottles used to measure the drift in the system. C. Diagram of the temperature map after 300 seconds of heating. The numbers correspond to the coil numbers.

Results: The maximum, mean and standard deviation of the error between the predicted and simulated local SAR maps was: 0.0060 %, 3.1710e-005 % and 3.8565e-004 %, respectively (Figure 1). In the phantom setting (Figure 4), the maximum, mean and standard deviation of temperature difference between the predicted and the measured temperature was 0.324, 0.00832 and 0.046 degrees C, respectively.

Conclusions: At ultra-high magnetic field strength, interactions between electromagnetic field and dielectric tissues may cause SAR hot-spots, potentially dangerous for patients. Knowledge of local SAR distribution is therefore a critical issue for ultra-high field applications. Current SAR monitoring techniques offer no capability for a-priori prediction of local SAR and are not suitable for testing transmit arrays or pulse sequences. In this study, we propose and validate a local SAR prediction model. Once the model is calibrated, the local SAR can be predicted for any RF pulse in the parallel transmit regime. The method also allows the prediction of the temperature change as long as the heating is occurs sufficiently rapidly and is linear. The method is a potential candidate for local SAR prediction in parallel Tx systems. It can be used to assess various coil and pulse designs and future work includes the extension of this model to in-vivo studies.

References: 1. Zhu Y. In Vivo RF Power and SAR Calibration for Multi-Port RF Transmission. ISMRM 09. 2. Lattanzi R. et al. Electrodynamic Constraints on Homogeneity and Radiofrequency Power Deposition in Multiple Coil Excitations. Magn Reson Med 2009; 61:315- 334. 3.Cline H. RadioFrequency Power Deposition Utilizing Thermal Imaging. Magn Reson Med 2004; 51:1129- 1137. 4. Alon L. et al. Automated In Vivo Global SAR prediction and monitoring for Parallel Transmission. ISMRM Parallel Workshop. Oct 09.